Effects of Amino Acid Substitutions at β131 on the Structure and Properties of Hemoglobin: Evidence for Communication between $\alpha_1\beta_1$- and $\alpha_1\beta_2$-Subunit Interfaces†

Chung-ke Chang,‡ Virgil Simplaceanu, and Chien Ho*

Department of Biological Sciences, Carnegie Mellon University, Pittsburgh, Pennsylvania 15213

Received October 11, 2001

ABSTRACT: Substitutions of Asn, Glu, and Leu for Gln at the β131 position of the hemoglobin molecule result in recombinant hemoglobins (rHbs) with moderately lowered oxygen affinity and high cooperativity compared to human normal adult hemoglobin (Hb A). The mutation site affects the hydrogen bonds present at the $\alpha_1\beta_1$-subunit interface between α103His and β131Gln as well as that between α122His and β35Tyr. NMR spectroscopy shows that the hydrogen bonds are indeed perturbed; in the case of rHb (β131Gln → Asn) and rHb (β131Gln → Leu), the perturbations are propagated to the other $\alpha_1\beta_1$-interface H-bond involving α122His and β35Tyr. Proton exchange measurements also detect faster exchange rates for both $\alpha_1\beta_1$-interface histidine side chains of the mutant rHbs in 0.1 M sodium phosphate buffer at pH 7.0 than for those of Hb A under the same conditions. In addition, the same measurements in 0.1 M Tris buffer at pH 7.0 show a much slower exchange rate for mutant rHbs and Hb A. One of the mutants, rHb (β131Gln → Asn), shows the conformational exchange of its interface histidines, and exchange rate measurements have been attempted. We have also conducted studies on the reactivity of the SH group of β93Cys (a residue located in the region of the $\alpha_1\beta_2$-subunit interface) toward *p*-mercuribenzoate, and our results show that low-oxygen-affinity rHbs have a more reactive β93Cys than Hb A in the CO form. Our results indicate that there is communication between the $\alpha_1\beta_1$- and $\alpha_1\beta_2$-subunit interfaces, and a possible communication pathway for the cooperative oxygenation of Hb A that allows the $\alpha_1\beta_1$-subunit interface to modulate the functional properties in conjunction with the $\alpha_1\beta_2$ interface is proposed.

Human normal adult hemoglobin (Hb A)[1] is one of the most studied proteins and serves as a paradigm for the structure−function relationship of multimeric, allosteric proteins. Hb A is a tetrameric protein of molecular mass ~64 500 daltons consisting of 2 identical α-chains with 141 amino acids each and 2 identical β-chains with 146 amino acids each. The binding of oxygen to Hb A is cooperative; i.e., the binding of the first oxygen molecule enhances binding of the second, third, and fourth oxygen molecules. Based on a comparison of the detailed structural features of Hb A in deoxy (T) and oxy (R) forms, Perutz and colleagues (*1*−*5*) have shown that there are two different types of subunit interfaces, namely, $\alpha_1\beta_1$ (or $\alpha_2\beta_2$) and $\alpha_1\beta_2$ (or $\alpha_2\beta_1$), and that during the transition from the deoxy to the oxy state, the $\alpha_1\beta_2$-subunit interface undergoes a sliding movement, while the $\alpha_1\beta_1$-subunit interface remains essentially unchanged. Subsequent research has thus focused on the $\alpha_1\beta_2$-subunit interface of hemoglobin (Hb), both to understand the molecular mechanism of its function (*6*) and to attempt the production of low-oxygen-affinity mutants, which might be useful as blood substitutes (*7*).

The discovery that naturally occurring Hb with mutations at the $\alpha_1\beta_1$-subunit interface can result in lowered oxygen affinity (*8*, *9*) sparked new interest in this interface. The mechanism of the lowered oxygen affinity of these mutants, Hb Presbyterian (β108Asn → Lys) and Hb Yoshizuka (β108Asn → Asp), has been attributed to electrostatic effects at the central cavity (*9*, *10*). A similar conclusion was reached for the recombinant form of these mutants (*10*). However, the later discovered Hb Schlierbach (β108Asn → Ile) (*11*) and recombinant hemoglobins (rHbs), rHb (β108Asn → Gln) (*12*) and rHb (β108Asn → Ala) (C.-H. Tsai and C. Ho, unpublished results), also show lower oxygen affinity than Hb A. The lowered oxygen affinity of these mutants cannot be explained by the central cavity theory alone; thus, other mechanisms must also play a role in modulating their functional properties.

Computational methods have suggested that the $\alpha_1\beta_1$-subunit interface plays a role in the T → R transition of Hb

† This work is taken in part from the Ph.D. Thesis of C.C. This work is supported by research grants from the National Institutes of Health (R01HL-24525, R01HL-58249, and S10RR-11248).

* Address correspondence to this author at the Department of Biological Sciences, Carnegie Mellon University, 4400 Fifth Ave., Pittsburgh, PA 15213. Telephone: 412-268-3395; FAX: 412-268-7083; E-mail: chienho@andrew.cmu.edu.

‡ Present address: Institute of Biomedical Sciences, Academia Sinica, Taipei 11529, Taiwan.

[1] Abbreviations: Hb A, human normal adult hemoglobin; rHb, recombinant hemoglobin; HbO_2, oxy-Hb; deoxy-Hb, deoxyhemoglobin; met-Hb, methemoglobin; NMR, nuclear magnetic resonance; HSQC, heteronuclear single quantum coherence; HMQC, heteronuclear multiple quantum coherence; NOE, nuclear Overhauser effect; NOESY, nuclear Overhauser effect spectroscopy; ppm, parts per million; DSS, 2,2-dimethyl-2-silapentane-5-sulfonate; Tris, tris(hydroxymethyl)aminomethane; 2,3-BPG, 2,3-bisphosphoglycerate; IHP, inositol hexaphosphate; PMB, *p*-mercuribenzoate.

10.1021/bi011919d CCC: $22.00
Published on Web 03/30/2002

A (*13, 14*). Experimental results from Ackers and colleagues (*15, 16*) also support the existence of favorable cooperativity between the α- and β-chains of the same dimer. A recent study shows that the $\alpha_1\beta_1$-interface histidines are destabilized in the deoxy state relative to the liganded state (*17*). Both tetramer−dimer dissociation studies (*18*) and NMR results where the T-state marker appears in low-oxygen-affinity $\alpha_1\beta_1$-interface mutants (*19*) suggest that changes at the $\alpha_1\beta_1$-subunit interface can propagate to the $\alpha_1\beta_2$-subunit interface.

In this study, we have introduced mutations at the β131 site, which is located at the $\alpha_1\beta_1$-subunit interface (*2, 5, 6*). The mutations affect the H-bond between α103His and β131Gln. These mutant rHbs show varied degrees of lowered oxygen affinity compared to Hb A. We have used nuclear magnetic resonance (NMR) spectroscopy on unlabeled and ^{15}N-labeled proteins to identify the $\alpha_1\beta_1$-interface histidines, and to measure their proton exchange rates at 15 °C. The reactivity of the SH group of β93Cys (a residue located at the $\alpha_1\beta_2$-subunit interface) with *p*-mercuribenzoate (PMB) was measured via a stopped-flow apparatus as a marker for the $\alpha_1\beta_2$-subunit interface. Our results indicate that mutations which affect the α103His also affect the dynamics of α122His, and that these changes can be propagated to the $\alpha_1\beta_2$-subunit interface. We also propose a general model by which interactions at the $\alpha_1\beta_1$-subunit interface can modulate the functional properties of hemoglobin.

MATERIALS AND METHODS

Construction of Expression Plasmids. The *Escherichia coli* Hb expression plasmid pHE2 was constructed in our laboratory as previously described (*20*). The β131 mutations were introduced into this plasmid between the *Pst*I and *Nhe*II restriction sites with the Muta-Gene phagemid kit from Bio-Rad. The synthetic oligonucleotides used to introduce the mutations are 5′-GCAACAACTTT*TTC*GTAAGCAG-CCT-3′ for rHb (β131Gln → Glu) (pHE274), 5′-GCAA-CAACTTT*GTT*GTAACGAGCCT-3′ for rHb (β131Gln → Asn) (pHE275), and 5′-GCAACAACTTT*CAG*GTAAG-CAGCCCT-3′ for rHb (β131Gln → Leu) (pHE2013), and were purchased from DNA International, Inc. (Lake Oswego, OR). Chemicals and restriction enzymes were purchased from major suppliers, such as Fisher, Sigma, Bio-Rad, Boehringer Mannheim, New England BioLabs, Pharmacia, Promega, Cambridge Isotope Laboratories, and United States Biochemicals, Inc., and were used without further purification. The desired mutations were confirmed by DNA sequencing.

Growth and Purification of rHbs. Growth and purification of rHbs followed the procedures described previously (*20, 21*). For rHb (β131Gln → Glu), the cells were lysed, and the supernatant from the lysate was left at 4 °C for 3 nights, after which the color of the supernatant became very red. For rHb (β131Gln → Asn) and rHb (β131Gln → Leu), the supernatants were left at 30 °C overnight. Uniformly ^{15}N-labeled rHbs were obtained by the method described by Simplaceanu et al. (*22*). The ^{15}N-labeled proteins were all left at 4 °C overnight. Following the procedure developed in our laboratory (*20, 21*), the rHb fraction collected after the Q-Sepharose Fast-Flow column (Pharmacia) was oxidized and reduced, and converted to the CO-liganded form. This Hb solution was then purified by eluting through a fast protein liquid chromatography Mono-S column (Pharmacia).

The rHbs were then checked with a VG Quattro-BQ (Fisions Instruments, VG Biotech, Altrincham, U.K.) electrospray ionization mass spectrometer as described in Shen et al. (*20*). Automated cycles of Edman degradation were performed on an Applied Biosystems gas/liquid-phase sequencer (model 470/900A) equipped with an on-line phenylthiohydantoin amino acid analyzer (model 120A). Except for unlabeled rHb (β131Gln → Glu), all rHbs used in this study had the correct molecular weights and contained less than 1% methionine at the amino termini. Unlabeled rHb (β131Gln → Glu) had 9% methionine.

Oxygen-Binding Properties of rHbs. Hb samples were exchanged with deionized water in a Centricon centrifugal concentrator with a molecular mass cutoff of 30 kDa (Centricon-30, Amicon, Inc.). The oxygen dissociation curves of rHbs were measured by a Hemox Analyzer (TCS Medical Products, Huntington Valley, PA) at 29 °C as a function of pH in 0.1 M sodium phosphate buffer. The concentration of Hb used for these measurements was around 0.1 mM per heme. The methemoglobin (met-Hb) reductase system was used as needed to reduce the amount of met-Hb in the sample (*23*). A visible absorption spectrum of each Hb sample was recorded immediately after oxygen equilibrium measurement, and the met-Hb content was estimated by using the extinction coefficient for Hb reported by Antonini (*24*). In the presence of the met-reductase system, the met-Hb content of the samples studied was below 2%. Oxygen equilibrium parameters were derived by fitting the Adair equations to each equilibrium oxygen-binding curve by a nonlinear least-squares procedure. P_{50}, a measure of oxygen affinity, was obtained at 50% O_2 saturation. The Hill coefficient (n_{max}), a measure of cooperativity, was determined from the maximum slope of the Hill plot by linear regression. n_{max} was derived between 60% and 65% oxygen saturation. The accuracy of P_{50} measurements (in mmHg) is ±5%, and that of n_{max} is ±7%.

Proton NMR Spectroscopy Investigation of rHbs. ^{1}H NMR spectra of rHbs were obtained from Bruker AVANCE DRX-300 and/or AVANCE DRX-600 spectrometers. All rHb samples were either in 0.1 M sodium phosphate buffer or in 0.1 M Tris buffer in the presence of 0.18 M Cl^- in H_2O. Some of the samples had 5−10% ^2H_2O added for the lock signal. The Hb concentration used for the experiments varied from 3% to 5% for the ^{15}N-labeled samples, and from 4% to 10% for the unlabeled samples. The water signal was suppressed by using either a jump-and-return sequence (*25*) or a selective shaped-power soft pulse sequence. Proton chemical shifts are referenced to the methyl proton resonance of 2,2-dimethyl-2-silapentane-5-sulfonate (DSS) indirectly by using the water signal, which occurs at 4.76 ppm downfield from that of DSS at 29 °C, as the internal reference. The nuclear Overhauser effect spectroscopy (NOESY) experiments and heteronuclear multiple-quantum coherence (HMQC) experiments were all carried out on a Bruker AVANCE DRX-600 instrument, and a 5-ms mixing time was used for the NOESY experiments. Processing of the 2D spectra was carried out with the XWinNMR package (Bruker) on a SGI workstation (Silicon Graphics Inc.).

Proton Exchange Measurements of rHbs and Hb A with Solvent. The proton exchange measurements were performed at 15 °C on a Bruker AVANCE DRX-600 spectrometer for the mutant rHbs and at both 15 °C and 37 °C for Hb A as

a control. Following the protocol of Mihailescu and Russu (*17*), the water proton resonance was selectively inverted with either a 2-ms or a 5-ms Gaussian 180° pulse, and the intensity of the Hb proton resonances was monitored as a function of the exchange delay (τ) after inversion. A weak gradient was applied during the delay τ to prevent the effects of radiation damping on the recovery of water magnetization to equilibrium. A modified jump-and-return sequence was used for the observation pulse. The magnetization of an exchangeable proton varies with the delay τ, and is described by the equation (*26*):

$$M(\tau) = M^0 + \{M(0) - M^0 - A\} \times e^{-(R_1+k)\tau} + A \times e^{-R_\omega \tau} \quad (1)$$

with

$$A = (q-1) \times \frac{k}{R_1 + k - R_w} \times M^0$$

where M^0 is the equilibrium magnetization, R_1 is the longitudinal relaxation rate, k is the exchange rate for the proton of interest, R_w is the longitudinal relaxation rate of water, and $q = M_w(0)/M_w^0$ expresses the efficiency of inversion of the water magnetization (e.g., $q = -1$ for perfect inversion).

Depending on the rate of exchange, either the full equation or its initial-rate approximation was used:

$$M(\tau) = M(0) - \{[M(0) - M^0] \times (R_1 + k) - (q-1)kM^0\}\tau \quad (2)$$

The magnetization of the exchangeable proton of interest was fitted as a function of exchange delay τ to either eq 1 or eq 2. $M(0)$ is left as an independent parameter in the fit to allow for the small uncertainty in the definition of the exchange delay resulting from the length of the inversion pulse on water. R_w and q were measured in separate experiments. ($R_1 + k$) values were measured in inversion recovery experiments in which each exchangeable proton resonance of interest was selectively inverted and its recovery over delays τ was monitored.

Conformational Exchange Measurement of the α*122His Resonances in rHb (*β*131Gln → Asn).* Based on a two-site system, and assuming (i) no cross-relaxation between the two conformations, (ii) similar longitudinal relaxation rates for the proton in both conformations, and (iii) equilibrium population obtainable by the intensity ratio between the resonances representing the two conformations, one is able to extract the conformational exchange rate using a 2D-NOESY spectrum (*26*). Assuming an equilibrium constant of around 2 [obtained by integrating the resonances at 12.9 and 12.1 ppm of rHb (β131Gln → Asn) in the CO form], the conformational exchange rate can be obtained by the equations:

$$\frac{I_{AB}}{I_{AA}} = \frac{1 - e^{-x}}{2 + e^{-x}} \quad (3)$$

$$\frac{I_{AB}}{I_{BB}} = \frac{2 - 2e^{-x}}{1 + 2e^{-x}} \quad (4)$$

where

$$x = 3\tau_m k_1 \quad (5)$$

and I_{AA} and I_{BB} are the intensities of the diagonal resonances for each conformer, and I_{AB} is the intensity of the exchange cross-peak between those two. k_1 is the forward exchange rate and k_{-1} the reverse exchange rate ($k_{-1} = 2k_1$). The relationship between k_{ex}, k_1, and k_{-1} is

$$k_{ex} = k_1 + k_{-1} \quad (6)$$

Reactivity Measurements of β*93Cys with p-Mercuribenzoate (PMB).* Reactivity studies were conducted on an OLIS stopped-flow apparatus (OLIS, Bogart, GA) with a dead time of ~3 ms. A circulating water bath, monitored with a thermometer, was used to keep the temperature at 20 °C. The light source was a deuterium lamp, and the reactions were monitored at 255 nm. Reactions were followed for 200−500 ms in the case of liganded rHbs and Hb A, and for 2−5 s in the case of deoxy-rHbs and deoxy-Hb A. A final heme concentration of 12.5 μM and a PMB concentration of 50 μM were used for all reactions. For reactions in the presence of inositol hexaphosphate (IHP), the final IHP concentration used was 1 mM. All reactants were prepared in 0.1 M potassium phosphate buffer at pH 7.0 according to Mathews et al. (*27*). For anaerobic operations, a 10-mL solution of degassed 0.1 M potassium phosphate buffer at pH 7.0 containing 10 mg of sodium dithionite was loaded into the stopped-flow system on the day before actual measurements. The water bath in the stopped-flow apparatus was bubbled with Ar gas overnight and during the measurements. Before the samples were loaded, a 15-mL solution of degassed 0.1 M potassium phosphate buffer at pH 7.0 was used to wash the stopped-flow system. All loading syringes were washed with Ar-saturated buffer just prior to usage. The pseudo-first-order rate constant was then obtained by fitting the experimental data with a single-exponential equation through a least-squares method.

RESULTS

Oxygen-Binding Studies of Hb A and Mutant rHbs. Table 1 is a summary of the oxygen-binding studies of the various rHbs and Hb A in 0.1 M sodium phosphate buffer at 29 °C, and the resulting plot is shown in Figure 1. We notice that all three mutant rHbs show lowered oxygen affinity while maintaining essentially normal cooperativity under these experimental conditions. While the differences in oxygen affinity among rHb (β131Gln → Glu), rHb (β131Gln → Asn), and Hb A are very small, rHb (β131Gln → Leu) does show a markedly lower oxygen affinity. The β131Gln → Glu mutation also occurs in nature [Hb Camden (β131Gln → Glu)], and previous reports stated it as having normal oxygen affinity compared to Hb A (*28*, *29*). While it is true that the differences are very small at any given data point, when looking at Figure 1 as a whole, it is clear that the slightly lowered oxygen affinity of rHb (β131Gln → Glu) over the pH ranges studied cannot be explained by experimental error alone.

Proton Resonances of α*103His and* α*122His in rHbs and Hb A.* The exchangeable proton resonances of α103His and α122His of the various mutant rHbs and Hb A in the CO

Table 1: Oxygen-Binding Data of Various β131 Mutant rHbs and Hb A in 0.1 M Sodium Phosphate Buffer at 29 °C

	pH	P_{50} (mmHg)	n_{max}
Hb A	6.74	22.2	3.2
	6.88	20.0	3.2
	7.08	15.9	3.2
	7.22	13.9	3.2
	7.41	10.5	3.3
	7.70	7.3	3.1
	8.04	5.1	3.0
rHb (βQ131E)	6.76	22.5	2.7
	6.95	19.0	2.8
	7.37	12.1	2.9
	7.63	9.4	3.0
	7.73	9.2	3.0
	7.94	7.0	2.8
	8.07	6.5	2.8
rHb (βQ131N)	6.22	30.8	2.9
	6.84	24.2	2.9
	7.04	19.2	3.2
	7.34	13.5	3.0
	7.40	13.9	3.0
	7.78	8.9	2.9
	8.14	5.6	3.1
rHb (βQ131L)	6.53	41.4	2.8
	6.79	33.9	2.9
	7.06	25.0	2.9
	7.36	17.4	3.3
	7.62	11.5	3.0
	7.86	8.9	3.0

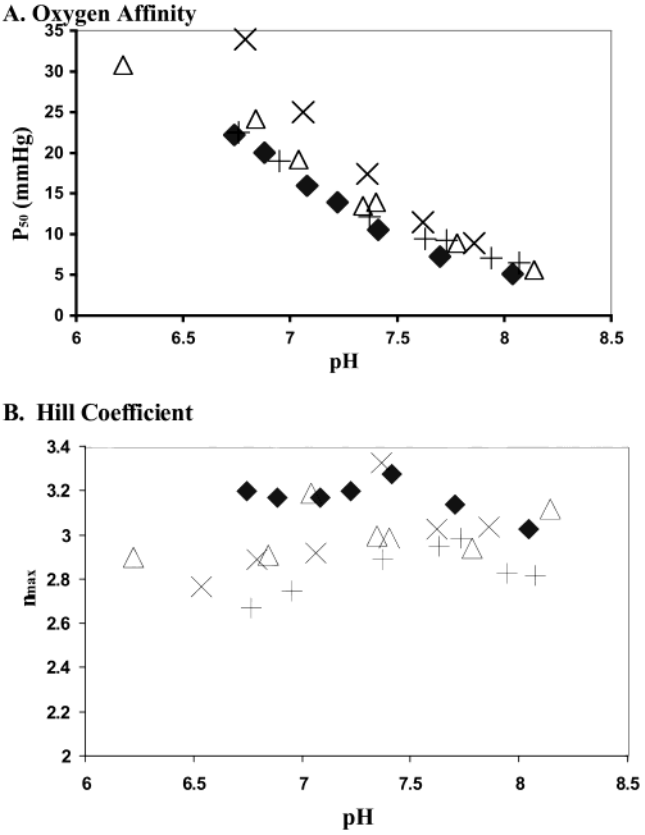

FIGURE 1: Oxygen affinity (P_{50}) (A) and the Hill coefficient (n_{max}) (B) in 0.1 M sodium phosphate buffer at 29 °C as a function of pH: (◆) Hb A; (+) rHb (β131Gln → Glu); (△) rHb (β131Gln → Asn); and (×) rHb (β131Gln → Leu). Oxygen dissociation data were obtained with 0.1 mM Hb and in the presence of a reductase system (*23*).

form at 15 °C are shown in Figure 2. In Hb A, the resonance at 12.2 ppm has been assigned to the side-chain $N_{\epsilon 2}H$ group of α103His, which is hydrogen-bonded to β131Gln (or to the peptide carbonyl of β108Asn) (*19, 22, 30, 31*). The resonance at 12.9 ppm has been assigned to the side-chain $N_{\epsilon 2}H$ group of α122His (*22*), which forms a water-mediated H-bond with the side chain of β35Tyr. Both H-bonds are located at the $\alpha_1\beta_1$-subunit interface of Hb A. It is clear in this figure that mutations at the β131 position can perturb both interface histidine resonances (α103His and α122His) and that the perturbations are not just confined to the mutation site. rHb (β131Gln → Glu) shows a slight downfield shift of the α122His resonance at 13.1 ppm, indicating that the Glu mutation at β131 can affect the environment of α122His. The nature of the bulge at 14 ppm in rHb (β131Gln → Glu) is unclear to us. In deoxy-Hb A, the resonance at 14 ppm has been assigned to the H-bond between α42Tyr and β99Asp (*32*), and used as a T-state marker. In other low-oxygen-affinity mutants, the appearance of the 14-ppm resonance in the liganded form is often taken as an indication of the presence of a T-like structure (*7, 33*). However, we observe only a slight decrease in the oxygen affinity of rHb (β131Gln → Glu). More research will be needed to elucidate the nature of this resonance in rHb (β131Gln → Glu).

The deoxy spectra of the mutant rHbs and Hb A under the same experimental conditions are shown in Figure 3. We can immediately observe the direct effect of mutating β131 on the α103His resonance. In rHb (β131Gln → Asn) and rHb (β131Gln → Leu), the effect extends to the α122His resonance, just as observed in the CO form. The α122His resonance in rHb (β131Gln → Leu) is shifted, thus indicating that it has been affected by the Leu mutation. rHb (β131Gln → Glu) shows no significant changes to the α122His resonance except for a slight downfield shift similar to that observed in the CO form. In Figure 4A, we show the proximal histidines observed at a lower magnetic field at 29 °C. The resonance at 63 ppm has been assigned to the hyperfine-shifted $N_\delta H$-exchangeable proton of α87His, while the resonance at 75 ppm has been assigned to the corresponding proton of β92His (*34, 35*). These resonances are indicative of the heme pocket environment of Hb. Here, we have observed slight shifts of the proximal histidine resonances in the mutant rHbs compared to Hb A. In Figure 4B, we show the ferrous hyperfine-shifted and exchangeable proton resonances under the same conditions as Figure 4A. The hyperfine-shifted resonances between 15 and 24 ppm are also slightly different in the mutant rHbs. These resonances have already been assigned to either the α- or the β-chains (*31*). Our results show that the differences are not limited to the β-chain resonances, suggesting that the mutations at β131 affect both the α- and β-heme pockets.

Assignment of the α122His and α103His Resonances in Mutant rHbs. The first question that we need to address is which resonance belongs to which interface histidine in the mutant rHbs. We have carried out proton−proton NOESY and heteronuclear ^1H-^{15}N correlation experiments on the various mutants in the CO form and attempted to determine the assignments by comparing the nuclear Overhauser effect (NOE) patterns of the mutants with those of Hb A. As shown in Figure 5, the NOE patterns of the cross-peaks between 6 and 8.5 ppm in Hb A are different for the α122His (12.9-ppm) and α103His (12.1-ppm) resonances. These cross-peaks should arise from the C2 and C4 protons of the histidyl

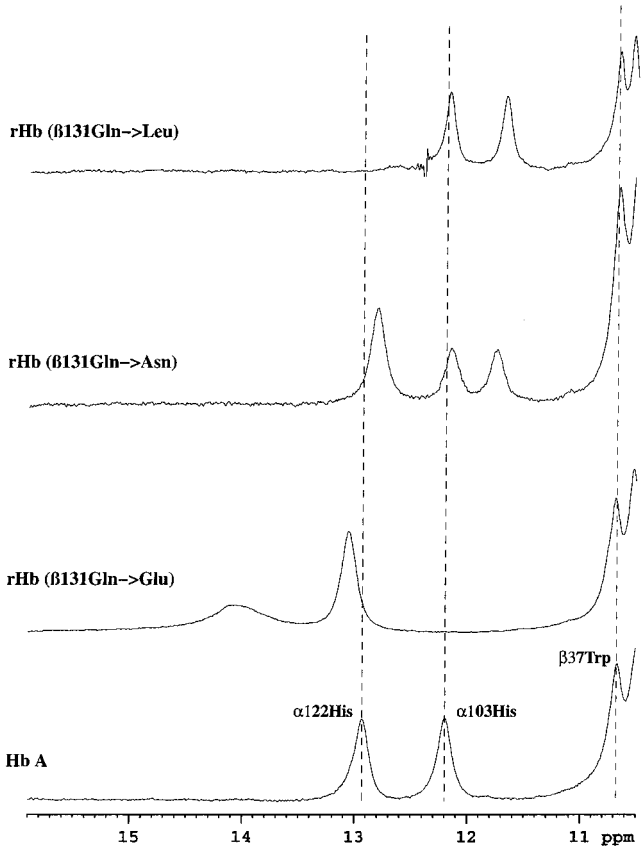

FIGURE 2: 600-MHz ^{1}H NMR spectra of the exchangeable proton resonances of Hb A and rHbs in the CO form in 0.1 M sodium phosphate buffer at pH 7.0 and 15 °C. The resonances marked by the dashed lines from left to right have been assigned to α122His, α103His, and *β*37Trp in Hb A, respectively.

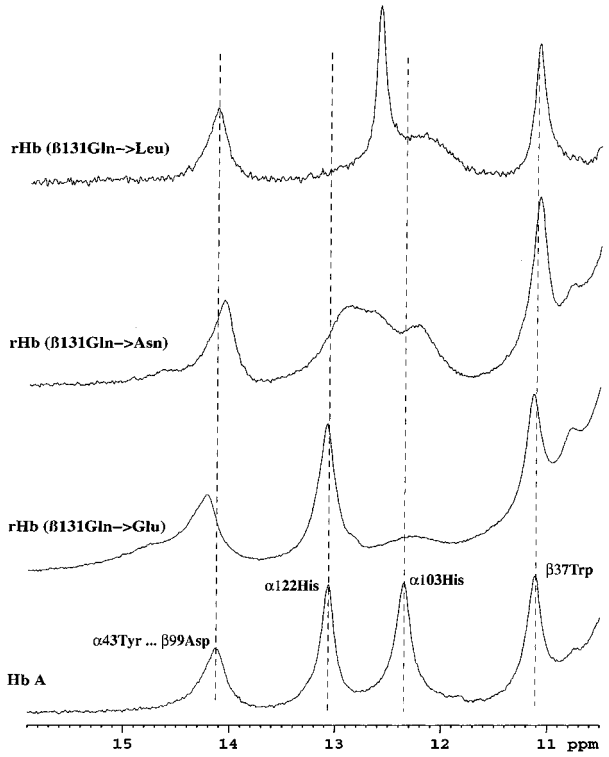

FIGURE 3: 600-MHz ^{1}H NMR spectra of the exchangeable proton resonances of Hb A and rHbs in the deoxy form in 0.1 M sodium phosphate buffer at pH 7.0 and 15 °C. The resonances marked by the dashed lines from left to right have been assigned to the H-bond between α42Tyr and *β*99Asp, α122His, α103His, and *β*37Trp in Hb A, respectively.

residue (*30*); due to the different environments between α122His (proximity to the aromatic ring of *β*35Tyr) and α103His, the cross-peaks show a different pattern confirmed by HMQC experiments. We can see from the same figure that the 13-ppm resonance of rHb (*β*131Gln → Glu), the 12.9- and 12.1-ppm resonances of rHb (*β*131Gln → Asn), and the 12.1-ppm resonance of rHb (*β*131Gln → Leu) all share the same pattern as the α122His resonance of Hb A at 12.9 ppm. They definitely belong to a histidyl side chain as shown in Figure 6. Thus, we propose that these resonances should be assigned to α122His. The strong cross-peaks (shown with an asterisk) between the 12.9- and 12.1-ppm resonances of rHb (*β*131Gln → Asn) arise from the proton sampling two alternative environments (discussed below).

Unfortunately, we could not observe mutant NOE patterns similar to the one observed for α103His in Hb A, except possibly for rHb (*β*131Glu → Leu). However, we suggest that the 11.7-ppm resonance of rHb (*β*131Gln → Asn) and the 11.6-ppm resonance of rHb (*β*131Gln → Leu) should be assigned to α103His. This is based on the following reasons: (i) According to the HMQC spectra of the various rHbs in the CO form shown in Figure 6, the aforementioned resonances appear in the usual range at which $\alpha_1\beta_1$-interface histidines are observed in Hb. (ii) There are only two interface histidyl residues per $\alpha\beta$-dimer, and since we can assign the α122His resonances directly from their NOE patterns, by elimination the resonances that are left in the region should belong to α103His. (iii) It is known that the α103His resonance has a faster proton exchange rate with solvent than α122His. Our proton exchange rate measurements (discussed below) show that the 11.7-ppm resonance of rHb (*β*131Gln → Asn) and the 11.6-ppm resonance of rHb (*β*131Gln → Leu) have much faster exchange rates with solvent than the other measurable resonances of their respective mutant rHbs.

Furthermore, Figure 6 shows a putative histidine resonance at (10.5 ppm ^{1}H, 158 ppm ^{15}N) in rHb (*β*131Gln → Asn). Its intensity, compared to the resonance at (11.7 ppm ^{1}H, 165 ppm ^{15}N), is similar to the intensity of the resonance at (12.9 ppm ^{1}H, 166 ppm ^{15}N) compared to the resonance at (12.4 ppm ^{1}H, 163.5 ppm ^{15}N). Based on these results, as well as the NOESY results (Figure 5), we propose that this histidine resonance arises from an alternative environment of α103His. This leads us to suggest that each interface histidyl residue in rHb (*β*131Gln → Asn) has two alternative conformations in the CO form.

Proton Exchange Rate Measurements. Table 2 summarizes our results on the proton exchange rate measurements of the interface histidine residues of the mutant rHbs and Hb A. We have conducted our experiments in either 0.1 M sodium phosphate buffer at pH 7.0 and 15 °C or 0.1 M Tris buffer in the presence of 0.18 M Cl^- at pH 7.0 and 15 °C. The overall differences between the CO and deoxy forms of the mutant rHbs generally agree with those reported previously (*17*); i.e., both α103His and α122His show faster exchange rates in the deoxygenated T-state than in the ligated R-state. The small number of cases where we see a slightly faster rate for α122His in the CO form could arise from experimental errors, where the noise in the spectra alone accounts for close to 3% error (overall errors due to curve-fitting are

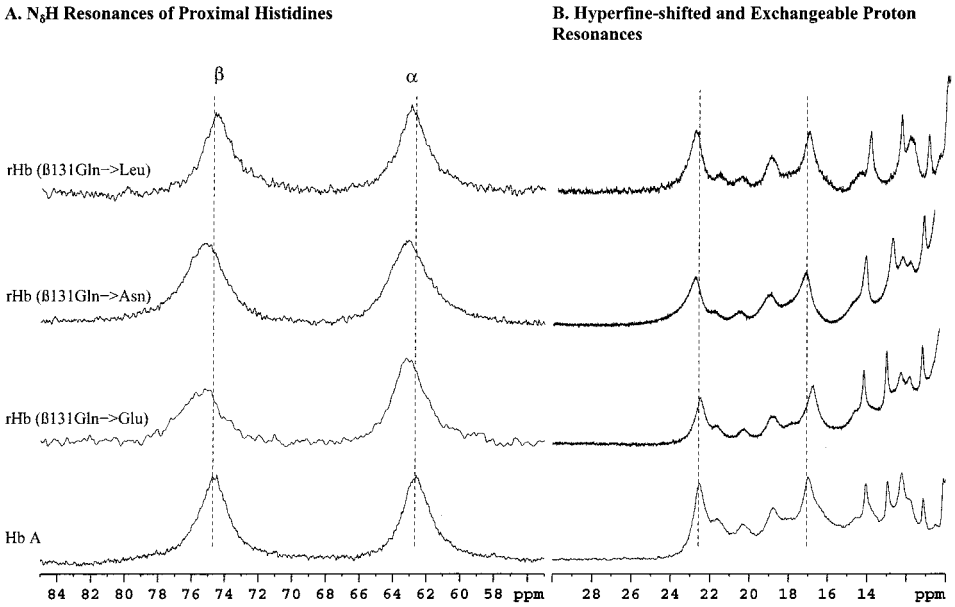

FIGURE 4: 300-MHz ^{1}H NMR spectra of hyperfine-shifted and exchangeable resonances of Hb A and rHbs in the deoxy form in 0.1 M sodium phosphate buffer at pH 7.0 and 29 °C: (A) ferrous hyperfine-shifted $N_\delta H$ resonances of proximal histidines; and (B) hyperfine-shifted and exchangeable proton resonances.

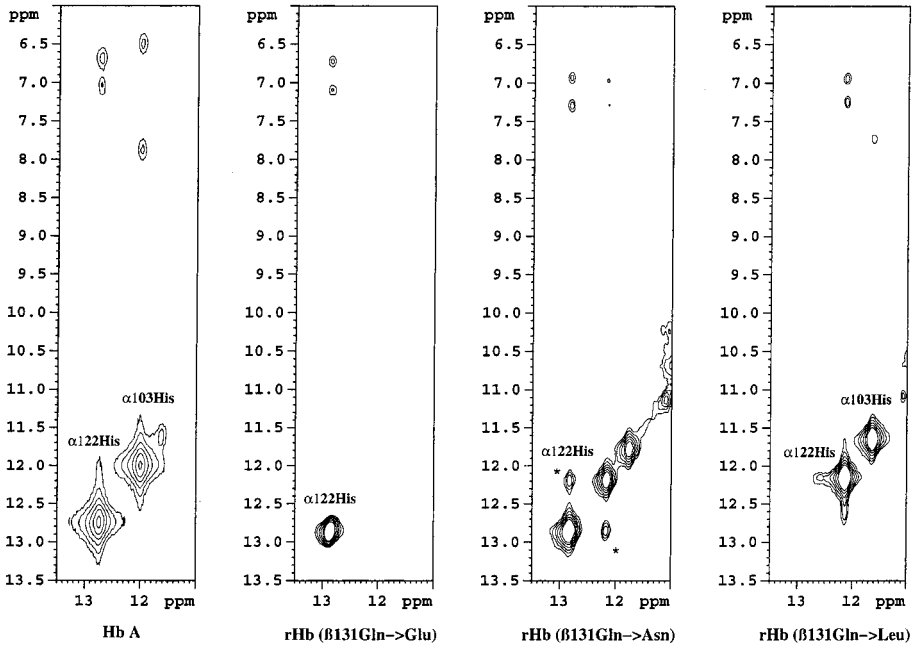

FIGURE 5: 600-MHz ^{1}H-^{1}H NOESY spectra of the interface histidyl residues of Hb A and rHbs in the CO form in 0.1 M sodium phosphate buffer at pH 7.0, and 15 °C.

on the order of 5−10%). We do see, however, a large impact of the buffer on the exchange rate. In 0.1 M phosphate buffer, it was often impossible to resolve some of the faster exchanging resonances, especially when the sample was in the deoxy form. Changing the buffer to 0.1 M Tris in the presence of 0.18 M Cl^- slows down the exchange enough for us to observe these fast-exchanging proton resonances, as shown in Figure 7. This effect is observed not only in the mutant rHbs but also in Hb A. In Table 2, we see that the exchange rates measured for Hb A in 0.1 M Tris in the presence of 0.18 M Cl^- at 15 °C are much slower than those measured in 0.1 M sodium phosphate at the same temperature. It should also be noted here that α103His seems to be more strongly affected by this choice of buffers than α122His, possibly due to the more compact environment of the latter.

Under the same ligation states and buffer conditions, we have observed faster exchange rates for both α103His and α122His in the mutant rHbs than in Hb A. This suggests that the $\alpha_1\beta_1$- and $\alpha_2\beta_2$-subunit interfaces of the mutant rHbs are more accessible to solvent, and thus they are more destabilized by the mutations. Again, we see that the mutation at β131 has effects on the α122His exchange rate, suggesting a structural interplay between these two $\alpha_1\beta_1$-interface sites.

Conformational Exchange Measurements of α122His in rHb (β131Gln → Asn). Since we could observe two conformations of α122His in rHbCO (β131Gln → Asn), we have attempted to measure the conformational exchange rate

Table 2: Proton Exchange Measurements of β131 Mutant rHbs and Hb A[a]

		CO form k_{ex} (s^{-1})		deoxy form k_{ex} (s^{-1})	
		α103His	α122His	α103His	α122His
0.1 M sodium phosphate, pH 7.0, 15 °C	Hb A	7	5	30	4
	rHb(βQ131E)	NA[b]	10	NA[e]	8
	rHb(βQ131N)	73	12[c] 16[d]	NA[e]	NA[e]
	rHb(βQ131L)	43	7	NA[f]	21
0.1 M Tris + 0.18 M Cl^-, pH 7.0, 15 °C	Hb A(37 °C)	11	7	38	9
	Hb A(15 °C)	6	5	8	4
	rHb(βQ131E)	NA[b]	8	NA[b]	8
	rHb(βQ131N)	26	12[c] 14[d]	36	19[c] 19[d]
	rHb(βQ131L)	11	7	44	8

[a] The accuracy of the experimental measurements is within ±10%. [b] The α103His resonance of rHb (β131Gln → Glu) is not observed in either the CO or the deoxy form spectra under our experimental conditions. [c] Numbers are for the downfield resonance, or "major" form of α122His. [d] Numbers are for the upfield resonance, or "minor" form of α122His. [e] The α103His resonances of rHb (β131Gln → Asn) are broadened beyond detection under this condition. [f] For rHb (β131Gln → Leu), the α103His resonance is broadened beyond detection under this condition.

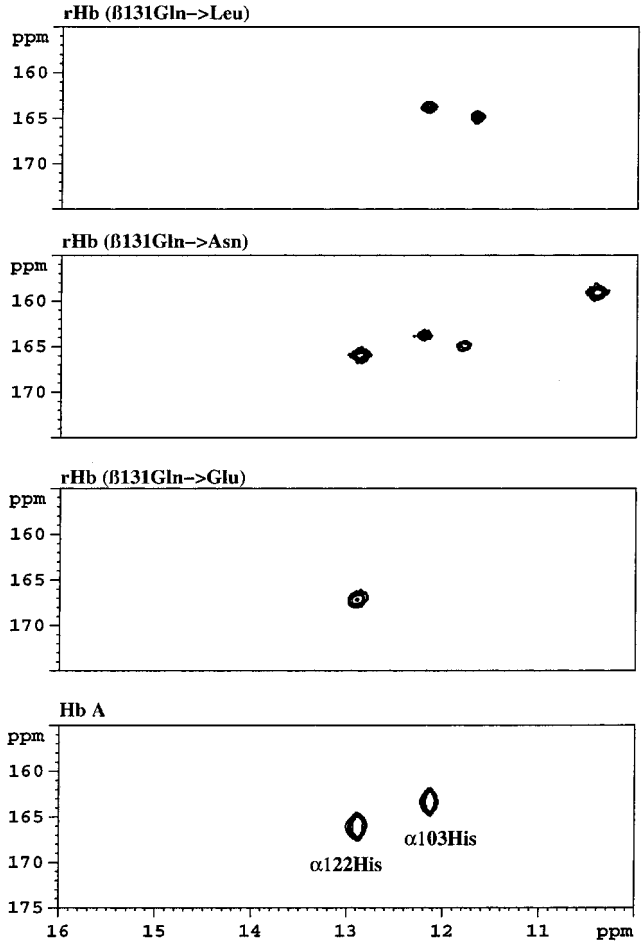

FIGURE 6: 600-MHz ^1H-^{15}N flip-back HMQC spectra of the interface histidyl residues of Hb A and rHbs in the CO form in 0.1 M sodium phosphate buffer at pH 7.0 and 15 °C.

of this mutant rHb. The results are shown in Table 3. We see that the numbers obtained under different τ_m agree fairly well with each other. The increase in temperature leads to an increase in the conformational exchange rate as expected. We were not able to measure the conformational exchange rate for α103His, probably because of the dominating effect of the faster exchange with the solvent protons. By correlating these results with those obtained from our HMQC experiments (Figure 6), we suggest that in the CO form the

Table 3: Conformational Exchange Measurements of α122His in the CO Form of rHb (β131Gln → Asn)

temp (°C)	τ_m (ms)	k_{ex} (s^{-1})
15	5	57
15	10	69
15	20	64
		avg 63 ± 6
29	5	161
29	10	141
		avg 151 ± 10

$\alpha_1\beta_1$ interface of rHb (β131Gln → Asn) is wobbling between two conformations at 15 °C. In the "major" conformation, the α122His−β35Tyr water-mediated H-bond is essentially unaltered relative to Hb A. The shorter side chain of Asn presumably disrupts the α103His−β131Gln H-bond ordinarily formed in Hb A, resulting in a more solvent-accessible environment. The weakening of the H-bond results in an upfield shift from 12.2 to 10.5 ppm in the proton dimension of the NMR spectrum. In the "minor" conformation, the Hb molecule attempts to form an H-bond between α103His and either the mutated side chain of β131Asn or the backbone carbonyl of β108Asn, which is less preferred in Hb A due to geometry issues. Such an attempt, however, puts a strain on the $\alpha_1\beta_1$ interface, which is propagated to the α122His site, thus probably weakening the original water-mediated H-bond between α122His and β35Tyr. This results in an upfield shift (to 12.1 ppm) of the α122His resonance. Also, if the attempt is successful, the α103His resonance regains some of its H-bond strength, and thus causes a downfield shift. This could explain why we observe the "minor" α103His resonance at 11.7 ppm. The coupled mechanism between the two $\alpha_1\beta_1$-interface histidines would also explain their relative intensities in the HMQC spectrum.

Studies of the Reactivity of β93Cys with PMB. Table 4 summarizes the results obtained from our β93Cys reactivity studies. PMB is a sulfhydryl reagent which reacts with the SH group of β93Cys in Hb A (*36*). In the deoxy form, β93Cys is protected by the salt-bridge formed between β94Asp and β146His, thus lowering its reactivity in relation to the liganded forms (*37, 38*). All samples show lowered reactivity in the deoxy form compared to the CO form with and without IHP, which is consistent with the above hypothesis. All the low-oxygen-affinity rHbs show higher

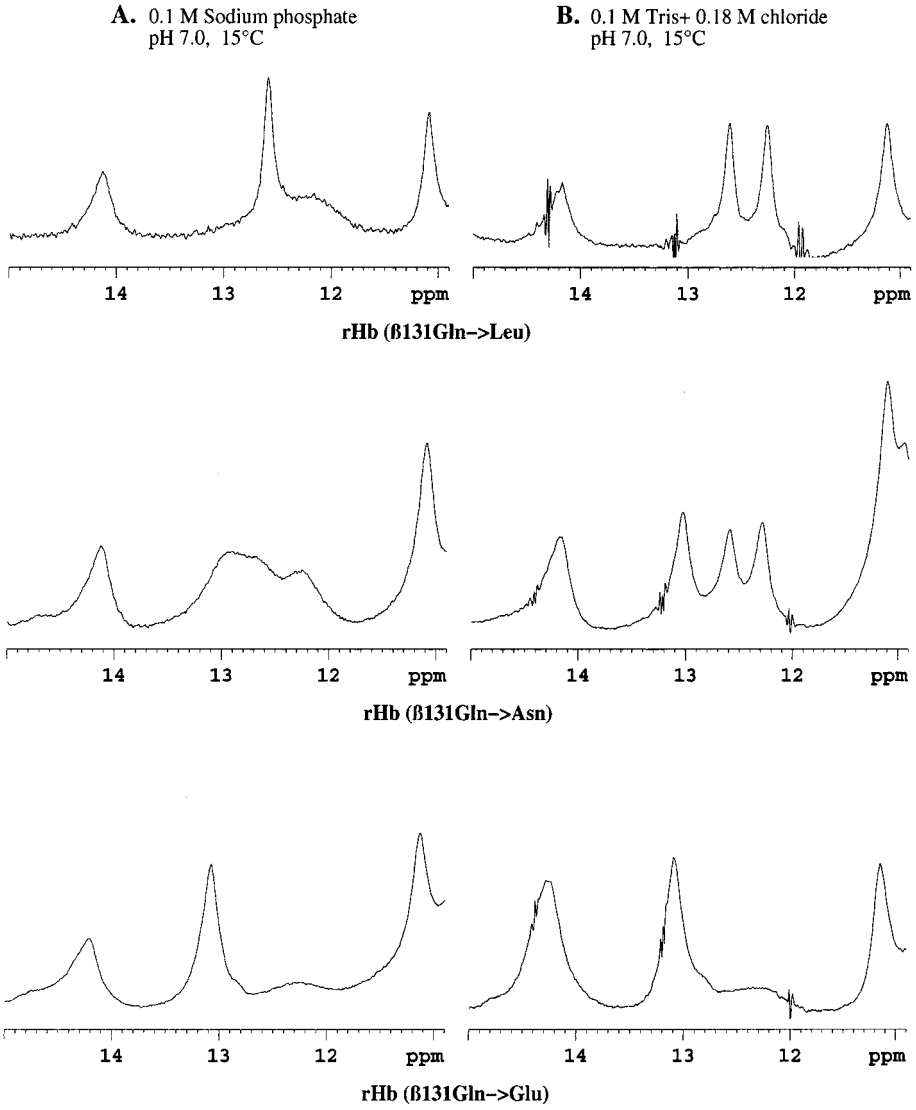

FIGURE 7: 600-MHz ^{1}H NMR spectra of rHbs in the deoxy form: (A) in 0.1 M sodium phosphate buffer at pH 7.0 and 15 °C; and (B) in 0.1 M Tris buffer + 0.18 M chloride at pH 7.0 and 15 °C.

Table 4: Pseudo-First-Order Rate Constants of Various rHbs Reacting with PMB at 20 °C in 0.1 M Potassium Phosphate Buffer at pH 7.0[a]

	CO form (s^{-1})	CO form + 1 mM IHP (s^{-1})	% change (+IHP/−IHP)	deoxy form (s^{-1})
Hb A	81	72	−12	1.7
low-oxygen-affinity rHbs				
rHb (βQ131E)	161	120	−26	1.8
rHb (βQ131N)	129	94	−27	1.5
rHb (βQ131L)	145	111	−23	1.8
rHb (βN108K)	167	85	−49	1.5
rHb (βN108A)	151	76	−50	1.3
rHb (αV96W)	154	66	−57	1.6
rHb (αV96W, βN108K)	211	72	−66	1.5
high-oxygen-affinity rHbs				
rHb Kempsey (βD99N)	40	44	+10	—[b]
rHb (αY42D, βD99N)	36	41	+14	—[b]
rHb (βC93A)	0	—	—	—

[a] The accuracy of the experimental measurements was within ±10%. [b] Values were not obtained due to our inability to completely deoxygenate the samples.

reactivity than Hb A in the CO form, while the high-oxygen-affinity rHbs tested in this study show lower reactivity under the same conditions. Upon addition of IHP while in the CO form, the low-oxygen-affinity rHbs show lower reactivity than in the absence of IHP. The magnitude of change seems to be related to the mutation site position. The high-oxygen-affinity rHbs show little change in reactivity when IHP is added. The increased reactivity of the low-oxygen-affinity rHbs represents increased accessibility of the β93Cys residue, and suggest a more open environment and/or increased mobility around β93Cys in the CO form. The results from the low-oxygen-affinity double mutant rHb (α96Val → Trp,

β108Asn → Lys) suggest some synergistic effect on the accessibility of β93Cys when two mutations are combined.

DISCUSSION

Ordered Water Molecules at the $\alpha_1\beta_1$-Subunit Interface. In rHb (β131Gln → Asn) and rHb (β131Gln → Leu), the mutations seem to propagate to the α122His site even though it is 7 Å away from the mutation site. The crystal structures of R, R2, and T structures of Hb A show a number of ordered water molecules at the $\alpha_1\beta_1$- and $\alpha_2\beta_2$-subunit interfaces (*4*, *5*, *39*, *40*). These water molecules are conserved throughout the R, R2, and T structures of Hb A (*40*). In Hb A, two conserved water molecules bridge the α103His residue to the α122His residue. The Asn and Leu mutations could destabilize this water network, thus leading to changes at the α122His environment. This interpretation is especially attractive considering that the water molecule participating in the water-mediated H-bond between α122His and β35Tyr is part of the network. According to Burnett et al. (*41*), polar to nonpolar or more bulky amino acid substitutions seem to have a larger destabilization effect on the ordered water molecules. Here, we see the same trend being propagated from the mutation site to the α122His environment, resulting in the large shift of the α122His resonance observed in rHb (β131Gln → Leu) (Figures 2 and 3). In rHb (β131Gln → Glu), we do not observe noticeable changes in the position of the α122His resonance (Figures 2 and 3); however, Table 2 shows that the exchange rate with solvent is still affected in this mutant rHb.

The destabilization of the $\alpha_1\beta_1$-interface water cluster could very well lead to changes in the functional properties of hemoglobin. It has been shown in *Scapharca* Hb that ordered water molecules act as allosteric mediators of this dimeric hemoglobin (HbI) (*42*). Furthermore, it has been reported that mutations destabilizing the water cluster in HbI alter its allosteric activity, although in this case they lead to a destabilized T-state, resulting in a high-oxygen-affinity phenotype (*43*). In Hb A, computer simulation studies have shown that ordered water molecules at the $\alpha_1\beta_1$-subunit interfaces can have an impact on the energetics of the allosteric transition (*41*). Mutations that affect interaction of the protein with ordered water have been shown to be responsible for changes in the oxygen affinity, like in the case of rHb (α96Val → Trp) (*44*). In the case of the $\alpha_1\beta_1$-subunit interface, it has been proposed that these mutants are more stable in the R-state than in the T-state (*17*). Destabilizing the water network at the $\alpha_1\beta_1$ interface in the R-state relative to the T-state should entice the Hb molecule to adopt a more T-like character, thus lowering its oxygen affinity. However, only rHb (β131Gln → Leu) shows an appreciable difference in oxygen affinity compared to Hb A. One possible explanation is that other interactions are countering the destabilization of the ordered water molecules (*41*). Another possible reason is that the destabilizing effect is not limited to the R-state; from Table 2 we see that the proton exchange rates of the mutant rHbs with solvent in both the CO and deoxy forms are affected. A combination of the two could lead to the only slightly lowered oxygen affinity observed for most cases in Table 1.

It should be noted that the mutation β35Tyr → Phe, which should affect the α122His environment directly, also shows slightly lowered oxygen affinity (*45*). In Figure 2 of that paper, the α103His resonance of deoxy-rHb (β35Tyr → Phe) at 12.2 ppm appears to be slightly broader than that of deoxy-Hb A, and there appear to be some changes in the relative intensities of the interface-histidine resonances in the liganded form of the mutant. This hints at the possibility of a two-way propagation pathway between the α103His environment and the α122His environment. Based on our present interpretation as described above, we speculate that the destabilization of the ordered water molecules at $\alpha_1\beta_1$-subunit interface brought about by the β35Tyr → Phe mutation is one of the factors responsible for the functional change. Recent crystallographic studies of β35 mutant rHbs (*46*) show changes in the water molecule network at the $\alpha_1\beta_1$-subunit interface, including increased mobility of the water molecule originally involved in the water-mediated H-bond between α122His and β35Tyr in Hb A.

Interaction between the $\alpha_1\beta_1$- and $\alpha_1\beta_2$-Subunit Interfaces. In Table 4, we used the reactivity of the SH group of β93Cys as an indicator of change at the $\alpha_1\beta_2$-subunit interface. It is evident that mutations at the $\alpha_1\beta_1$-subunit interface have an impact on the $\alpha_1\beta_2$-subunit interface. If we take the CO-form and deoxy-form reactivity constants of the various low-oxygen-affinity mutants as a basis, and assume that the addition of IHP forces the molecule toward the T-type structure, our results from rHb (α96Val → Trp), rHb (β108Asn → Lys), and rHb (α96Val → Trp, β108Asn → Lys) give us the following trends: (i) The three mutant rHbs mentioned above have a higher tendency to stay in the T structure upon addition of IHP. (ii) In the double-mutant rHb (α96Val → Trp, β108Asn → Lys), the stabilization effect on the T structure induced by the α96Val → Trp mutation on the β108Asn → Lys mutation is additive. These trends are essentially the same as observed by Tsai et al. (*19*).

On the other hand, the β131-mutant rHbs show more moderate changes in β93Cys reactivity, which is in good agreement with the general trend that the β131-mutant rHbs have less impact on the oxygen affinity of the Hb molecule. The sole exception, rHb (β131Gln → Leu), exhibits low-oxygen-affinity characteristics comparable to those of the β108-mutant rHbs (*12*, *19*), while maintaining the reactivity profile of the β131-mutant rHbs (Table 4). Considering the rather extreme mutation of rHb (β131Gln → Leu) and its dramatic effect on the $\alpha_1\beta_1$-subunit interface (Figures 2 and 3), other pathways are probably involved in modulating the oxygen affinity of this mutant.

Surprisingly, the high-oxygen-affinity rHb Kempsey (β99Asp → Asn) and rHb (α42Tyr → Asp, β99Asp → Asn) show *decreased* reactivity of their β93Cys-SH groups in the CO form (Table 4). We can interpret this result as a less mobile or less open β93Cys environment, thus reducing the SH group reactivity in these mutant rHbs. Coupled with the broken T-state H-bond between α42Tyr and β99Asn, it could explain the high oxygen affinity of the mutants. A "tighter" environment around β93Cys, which is located on the F helix of the β-chain, could also explain the delayed motion of the H helix and slower formation of the α42Tyr-β99Asp/Asn H-bond compared to Hb A (*47*) by representing a larger constraint on the motion of adjacent parts of the Hb molecule. The effect of IHP on the reactivity of β93Cys in these two mutant rHbs in the CO form is small.

The results from the β108 and β131 mutant rHbs provide additional evidence that there is communication between the $\alpha_1\beta_1$- and $\alpha_1\beta_2$-subunit interfaces. The fact that the results from the high-oxygen-affinity mutant rHbs show the reverse trend from the low-oxygen-affinity mutant rHbs also points to the possibility of using this reactivity assay as a fast and easy way to screen for low-oxygen-affinity rHbs. Although the exact mechanism of such a trend cannot be inferred from these results alone, it is clear that the accessibility of β93Cys-SH in the R-state is an important indicator of the oxygen affinity of the mutant rHbs.

Conformational Exchange of the $\alpha_1\beta_1$-Interface Histidines in the CO Form of rHb (β131Gln → Asn). The four resonances that appear at the interface histidine region of rHb (β131Gln → Asn) in the CO form (Figure 6) pose two interesting questions: (i) why do four resonances appear in this mutant; and (ii) how do they affect the functional properties of Hb? We have already suggested under Results a possible mechanism as an answer to the first question. The second question is more difficult to answer, mainly because we do not have enough information to show that the conformational exchange is affecting the function of this mutant rHb. Many of the functional experiments (Tables 1 and 4) carried out for this mutant in the current study show no significant differences between it and rHb (β131Gln → Glu), which does not show the conformational exchange phenomenon for the interface histidines.

If the conformational exchange of α103His and α122His is coupled as we propose, there is the possibility that the entire $\alpha_1\beta_1$-subunit interface is involved in this exchange. We think that at least in the CO form, by relaxing the interface interactions, an alternative interface conformation could become available to the molecule. It is interesting to note that rHbCO (β131Gln → Leu) has an interface histidine resonance profile very similar to that of the "minor" form resonances of rHbCO (β131Gln → Asn) in Figure 6. This could be interpreted as a complete switch of the $\alpha_1\beta_1$-subunit interface of rHb (β131Gln → Leu) to the alternative conformation in the CO form.

Buffer Effects on Proton Exchange Measurements. Different buffer systems seem to have an effect on the proton exchange rate of the $\alpha_1\beta_1$-interface histidines (Table 2 and Figure 7). By changing from phosphate buffer to Tris buffer with chloride, we are able to slow the proton exchange rate of α103His and α122His. It has been reported that phosphate exerts a larger allosteric effect than Tris with chloride (*48*); thus, the former lowers the oxygen affinity of Hb A more than the latter (*49*). The fact that we see a change in the proton exchange rate in different buffers that affect the oxygen affinity of hemoglobin strongly suggests a connection between these two properties. The increase in proton exchange rate of the interface histidines also suggests that the interface is more mobile in phosphate buffer. It has been shown that anions can affect the tertiary structure around the ligand-binding site of hemoglobin in the R-state (*50*). Among the inorganic anions, phosphate has a bigger effect than chloride. Molecular dynamics studies have linked the distal heme pocket of met-Hb with the $\alpha_1\beta_1$-subunit interface (*14*). It is possible that we are observing a manifestation of this linkage caused by the change of buffer.

Implication for Hemoglobin Structure and Function. Taken together, our results show that it is possible to moderate the oxygen affinity of hemoglobin by introducing mutations that change the dynamic properties of the $\alpha_1\beta_1$-subunit interface. Whereas the $\alpha_1\beta_1$-subunit interface is destabilized in the unliganded state, the $\alpha_1\beta_2$-subunit interface seems to show a reversed behavior. A comparison of the T, R, and R2 structures of Hb A has shown that the $\alpha_1\beta_2$-subunit interface is "tighter" in the T structure than in either R or R2 structures (*51*), and β37Trp, which is located in the hinge region of the $\alpha_1\beta_2$ interface, has been suggested to be stabilized in unliganded Hb A (*52*). In the T-state, mutations that introduce new interactions at the $\alpha_1\beta_2$-subunit interface can lower the oxygen affinity (*7, 44*), while those that disrupt interactions tend to raise it, but these results can be partly reversed by introducing a second mutation at the $\alpha_1\beta_2$-subunit interface (*53*). The interactions at the $\alpha_1\beta_1$-subunit interface seem to counteract the interactions at the $\alpha_1\beta_2$-subunit interface during the allosteric transition.

Results from Ackers and co-workers (*16, 54*) imply the existence of favorable cooperativity between the α- and β-hemes within the same $\alpha\beta$ dimer. Mihailescu and Russu (*17*) suggested that the $\alpha_1\beta_1$-subunit interface is involved in this energetic coupling. Structures of the $\alpha\beta$ dimer that are conformationally invariant between the deoxy and oxy forms of hemoglobin have been identified through analysis of existent crystal structures (*13*). These invariant structures have been suggested to play a role in communicating structural changes between the hemes, and the $\alpha_1\beta_1$-subunit interface plays an important role in this communication pathway. Ramadas and Rifkind (*14*) have further linked changes at the distal heme pockets of a methemoglobin $\alpha\beta$ dimer with dynamic fluctuations at the $\alpha_1\beta_1$- and $\alpha_2\beta_2$-subunit interfaces.

In the β131 mutant rHbs, the disruption at the $\alpha_1\beta_1$-subunit interface would result in a partial decoupling of the cooperative pathway within the $\alpha\beta$ dimer. According to Acker's symmetry rule model, such a decoupling should not incur a large penalty on the cooperativity of the rHb because most of the cooperativity originates from the binding of oxygen across the dimer interface (*16, 54*). Disruption of communication between the α- and β-chains within the dimer should moderately affect the oxygen affinity of the rHb, since the enhanced binding brought about by the intradimer cooperativity will be attenuated. Such a mechanism is in line with what we have observed in Figure 1, with the exception of rHb (β131Gln → Leu), where the nature of the amino acid substitution could introduce other factors that affect its functional properties.

Based on our present findings and other published results (*1, 14, 22, 54*), we propose a possible signal communication pathway for the cooperative oxygenation of hemoglobin [for details, see (*55*)]. Upon the binding of the first O_2 molecule to the Hb molecule, changes can be propagated to the $\alpha_1\beta_1$-subunit interface through proximal heme pocket interactions. At the same time, interactions propagating from the distal side of the heme pocket are communicated to the distal heme pocket of the adjacent subunit within the same $\alpha\beta$ dimer through a modulation of $\alpha_1\beta_1$-interface dynamics, since the two subunit interfaces share a number of amino acid residues, e.g., at the G helices (*6*). The second O_2-binding event on the same $\alpha\beta$ dimer then affects the remaining $\alpha_1\beta_1$-interface interactions. At this point, the $\alpha_1\beta_2$-interface interactions have been weakened to the point where the $\alpha_1\beta_1$-interface interac-

tions can now overpower them. This results in a further increase in affinity for the third O_2 molecule, and when it binds to the hemoglobin molecule, it activates the transition to the R structure. The fourth O_2 molecule then binds to an essentially high-affinity structure.

It is quite clear that there are long-range relationships among various parts of the Hb tetramer (*56*, *57*). Much effort has been focused on the $\alpha_1\beta_2$-subunit interface, since according to crystallographic results most of the structural changes during the T → R transition occur at this particular interface. Most of the analyses based on those results start out by treating the Hb molecule as a dimer of dimers. One must not forget, however, that the four chains of hemoglobin are in a tetrahedral arrangement, and thus changes at any one chain could potentially affect the other three. Our results allow us to reach the following conclusions: (i) mutations at β131 affect the proton exchange rate of both $\alpha_1\beta_1$-interface histidyl residues; (ii) these changes can have structural consequences on the $\alpha_1\beta_1$-subunit interface; and (iii) the overall effect of these changes can alter the functional properties of the Hb molecule. We also propose that the $\alpha_1\beta_1$-interface interactions might counteract the $\alpha_1\beta_2$-interface interactions, thus playing a part in the allosteric mechanism of hemoglobin. The present results provide further support to our early suggestion that allosteric interactions have multiple pathways for signal transmission in allosteric proteins (*19*, *58*−*60*). Our results further illustrate that hemoglobin is a rather flexible or adaptable molecule whose conformation can be adjusted in response to various perturbations (amino acid substitutions, binding of ligands and/or allosteric effectors, etc.) consistent with the "induced fit" model first proposed by Koshland and co-workers (*61*, *62*).

ACKNOWLEDGMENT

We thank Dr. Ming F. Tam for carrying out the mass spectrometric and Edman degradation analyses of our rHb samples, Dr. Yi Cheng for providing a sample of rHb (β93Cys → Ala), Dr. Ching-Hsuan Tsai for providing us samples of low-oxygen-affinity rHbs, Ms. Ming Zou and Ms. Nancy T. Ho for technical assistance, and Dr. Jonathan A. Lukin and Dr. E. Ann Pratt for helpful discussions.

REFERENCES

1. Perutz, M. F. (1970) *Nature 228*, 726−739.
2. Baldwin, J., and Chothia, C. (1979) *J. Mol. Biol. 129*, 175−220.
3. Baldwin, J. M. (1980) *J. Mol. Biol. 136*, 103−128.
4. Shaanan, B. (1983) *J. Mol. Biol. 171*, 31−59.
5. Fermi, G., Perutz, M. F., Shaanan, B., and Fourme, R. (1984) *J. Mol. Biol. 175*, 159−174.
6. Dickerson, R. E., and Geis, I. (1983) *Hemoglobin: structure, function, evolution, and pathology*, Benjamin/Cummings Publishing Co., Menlo Park, CA.
7. Kim, H. W., Shen, T. J., Sun, D. P., Ho, N. T., Madrid, M., and Ho, C. (1995) *J. Mol. Biol. 248*, 867−882.
8. Moo-Penn, W. F., Wolff, J. A., Simon, G., Vacek, M., Jue, D. L., and Johnson, M. H. (1978) *FEBS Lett. 92*, 53−56.
9. O'Donnell, J. K., Birch, P., Parsons, C. T., White, S. P., Okabe, J., Martin, M. J., Adams, C., Sundarapandiyan, K., Manjula, B. N., Acharya, A. S., et al. (1994) *J. Biol. Chem. 269*, 27692−27699.
10. Bonaventura, C., Arumugam, M., Cashon, R., Bonaventura, J., and Moo-Penn, W. F. (1994) *J. Mol. Biol. 239*, 561−568.
11. Frischknecht, H., Speich, R., Bloch, K. E., Fehr, J., Tuchschmid, P., and Jenni, R. (1999) *Hemoglobin 23*, 83−87.
12. Tsai, C.-H., Fang, T. Y., Ho, N. T., and Ho, C. (2000) *Biochemistry 39*, 13719−13729.
13. Nichols, W. L., Zimm, B. H., and Ten Eyck, L. F. (1997) *J. Mol. Biol. 270*, 598−615.
14. Ramadas, N., and Rifkind, J. M. (1999) *Biophys. J. 76*, 1796−1811.
15. LiCata, V. J., Dalessio, P. M., and Ackers, G. K. (1993) *Proteins: Struct., Funct., Genet. 17*, 279−296.
16. Ackers, G. K., Holt, J. M., Huang, Y., Grinkova, Y., Klinger, A. L., and Denisov, I. (2000) *Proteins Suppl. 4*, 23−43.
17. Mihailescu, M. R., and Russu, I. M. (2001) *Proc. Natl. Acad. Sci. U.S.A. 98*, 3773−3777.
18. Fronticelli, C., Gattoni, M., Lu, A. L., Brinigar, W. S., Bucci, J. L., and Chiancone, E. (1994) *Biophys. Chem. 51*, 53−57.
19. Tsai, C.-H., Shen, T. J., Ho, N. T., and Ho, C. (1999) *Biochemistry 38*, 8751−8761.
20. Shen, T. J., Ho, N. T., Simplaceanu, V., Zou, M., Green, B. N., Tam, M. F., and Ho, C. (1993) *Proc. Natl. Acad. Sci. U.S.A. 90*, 8108−8112.
21. Shen, T. J., Ho, N. T., Zou, M., Sun, D. P., Cottam, P. F., Simplaceanu, V., Tam, M. F., Bell, D. A., Jr., and Ho, C. (1997) *Protein Eng. 10*, 1085−1097.
22. Simplaceanu, V., Lukin, J. A., Fang, T. Y., Zou, M., Ho, N. T., and Ho, C. (2000) *Biophys. J. 79*, 1146−1154.
23. Hayashi, A., Suzuki, T., and Shin, M. (1973) *Biochim. Biophys. Acta 310*, 309−316.
24. Antonini, E. (1965) *Physiol. Rev. 45*, 123−170.
25. Plateau, P., and Guéron, M. (1982) *J. Am. Chem. Soc. 104*, 7310−7311.
26. Ernst, R. R., Bodenhausen, G., and Wokaun, A. (1988) *Principles of nuclear magnetic resonance in one and two dimensions*, Clarendon Press, Oxford University Press, Oxford, England.
27. Mathews, A. J., Olson, J. S., Renaud, J. P., Tame, J., and Nagai, K. (1991) *J. Biol. Chem. 266*, 21631−21639.
28. Cohen, P. T., Yates, A., Bellingham, A. J., and Huehns, E. R. (1973) *Nature 243*, 467−468.
29. Hubbard, M., Wilson, J. B., Wrightstone, R. N., Efremov, G. D., and Huisman, T. H. (1975) *Acta Haematol. 54*, 53−58.
30. Russu, I. M., Ho, N. T., and Ho, C. (1987) *Biochim. Biophys. Acta 914*, 40−48.
31. Ho, C. (1992) *Adv. Protein Chem. 43*, 153−312.
32. Fung, L. W., and Ho, C. (1975) *Biochemistry 14*, 2526−2535.
33. Ho, C., Sun, D. P., Shen, T. J., Ho, N. T., Zou, M., Hu, C.-K., Sun, Z.-Y., and Lukin, J. A. (1998) in *Present and Future Perspectives of Blood Substitutes* (Tsuchida, E., Ed.) pp 281−296, Elsevier Science SA, Lausanne, Switzerland.
34. Takahashi, S., Lin, A. K., and Ho, C. (1980) *Biochemistry 19*, 5196−5202.
35. La Mar, G. N., Nagai, K., Jue, T., Budd, D. L., Gersonde, K., Sick, H., Kagimoto, T., Hayashi, A., and Taketa, F. (1980) *Biochem. Biophys. Res. Commun. 96*, 1172−1177.
36. Antonini, E., and Brunori, M. (1969) *J. Biol. Chem. 244*, 3909−3912.
37. Gibson, Q. H. (1973) *J. Biol. Chem. 248*, 1281−1284.
38. Perutz, M. F., Kilmartin, J. V., Nagai, K., Szabo, A., and Simon, S. R. (1976) *Biochemistry 15*, 378−387.
39. Silva, M. M., Rogers, P. H., and Arnone, A. (1992) *J. Biol. Chem. 267*, 17248−17256.
40. Vasquez, G. B., Ji, X., Fronticelli, C., and Gilliland, G. L. (1998) *Acta Crystallogr., Sect. D: Biol. Crystallogr. 54 (Pt. 3)*, 355−366.
41. Burnett, J. C., Botti, P., Abraham, D. J., and Kellogg, G. E. (2001) *Proteins: Struct., Funct., Genet. 42*, 355−377.
42. Royer, W. E., Jr., Pardanani, A., Gibson, Q. H., Peterson, E. S., and Friedman, J. M. (1996) *Proc. Natl. Acad. Sci. U.S.A. 93*, 14526−14531.
43. Pardanani, A., Gambacurta, A., Ascoli, F., and Royer, W. E., Jr. (1998) *J. Mol. Biol. 284*, 729−739.
44. Puius, Y. A., Zou, M., Ho, N. T., Ho, C., and Almo, S. C. (1998) *Biochemistry 37*, 9258−9265.

45. Nakatsukasa, T., Nomura, N., Miyazaki, G., Imai, K., Wada, Y., Ishimori, K., Morishima, I., and Morimoto, H. (1998) *FEBS Lett. 441*, 93−96.
46. Kavanaugh, J. S., Weydert, J. A., Rogers, P. H., Arnone, A., Hui, H. L., Wierzba, A. M., Kwiatkowski, L. D., Paily, P., Noble, R. W., Bruno, S., and Mozzarelli, A. (2001) *Protein Sci. 10*, 1847−1855.
47. Hu, X., Rodgers, K. R., Mukerji, I., and Spiro, T. G. (1999) *Biochemistry 38*, 3462−3467.
48. Weber, R. E. (1992) *J. Appl. Physiol. 72*, 1611−1615.
49. Benesch, R. E., Benesch, R., and Yu, C. I. (1969) *Biochemistry 8*, 2567−2571.
50. Lindstrom, T. R., and Ho, C. (1973) *Biochemistry 12*, 134−139.
51. Srinivasan, R., and Rose, G. D. (1994) *Proc. Natl. Acad. Sci. U.S.A. 91*, 11113−11117.
52. Mihailescu, M. R., Fronticelli, C., and Russu, I. M. (2001) *Proteins: Struct., Funct., Genet. 44*, 73−78.
53. Kim, H. W., Shen, T. J., Sun, D. P., Ho, N. T., Madrid, M., Tam, M. F., Zou, M., Cottam, P. F., and Ho, C. (1994) *Proc. Natl. Acad. Sci. U.S.A. 91*, 11547−11551.
54. Ackers, G. K. (1998) *Adv. Protein Chem. 51*, 185−253.
55. Chang, C.-K. (2001) *Characterization of β131 Mutants of Hemoglobin: Effects on Hemoglobin Structure and Function*, Ph.D. Thesis, Carnegie Mellon Univeristy, Pittsurgh, PA.
56. Dumoulin, A., Manning, L. R., Jenkins, W. T., Winslow, R. M., and Manning, J. M. (1997) *J. Biol. Chem. 272*, 31326−31332.
57. Dumoulin, A., Padovan, J. C., Manning, L. R., Popowicz, A., Winslow, R. M., Chait, B. T., and Manning, J. M. (1998) *J. Biol. Chem. 273*, 35032−35038.
58. Barrick, D., Ho, N. T., Simplaceanu, V., Dahlquist, F. W., and Ho, C. (1997) *Nat. Struct. Biol. 4*, 78−83.
59. Sun, D. P., Zou, M., Ho, N. T., and Ho, C. (1997) *Biochemistry 36*, 6663−6673.
60. Barrick, Ho, N. T., Simplaceanu, V., and Ho, C. (2001) *Biochemistry 40*, 3780−3795.
61. Koshland, D. E., Jr. (1958) *Proc. Natl. Acad. Sci. U.S.A. 44*, 98−104.
62. Koshland, D. E., Jr., Nemethy, G., and Filmer, D. (1966) *Biochemistry 5*, 365−385.

BI011919D